



**HAL**  
open science

## Classification performances of Mine Hunting Sonar : Theory, practical results and operational applications

Franck Florin, François van Zeebroeck, Isabelle Quidu, Naig Le Bouffant

### ► To cite this version:

Franck Florin, François van Zeebroeck, Isabelle Quidu, Naig Le Bouffant. Classification performances of Mine Hunting Sonar : Theory, practical results and operational applications. Undersea Defence Technology (UDT) Europe 2003, Jun 2003, Malmö, Sweden. hal-00504857

**HAL Id: hal-00504857**

**<https://hal.science/hal-00504857>**

Submitted on 21 Jul 2010

**HAL** is a multi-disciplinary open access archive for the deposit and dissemination of scientific research documents, whether they are published or not. The documents may come from teaching and research institutions in France or abroad, or from public or private research centers.

L'archive ouverte pluridisciplinaire **HAL**, est destinée au dépôt et à la diffusion de documents scientifiques de niveau recherche, publiés ou non, émanant des établissements d'enseignement et de recherche français ou étrangers, des laboratoires publics ou privés.

# Classification performances of Mine Hunting Sonar : theory, practical results and operational applications

F. Florin F. Van Zeebroeck I. Quidu N. Le Bouffant

Thales Underwater Systems  
Route de Sainte Anne du Portzic, 29601 Brest cedex, France  
Tel: (33) 2 98 31 37 00  
E\_mail: Franck.Florin@fr.thalesgroup.com

## Abstract

As low target strength objects can be detected by the new generation of mine hunting sonar systems, more and more non mine like objects are passed on to the classification process. In the past, the mine hunting performance was mainly driven by the performance of the mine detector. With this improved detection capability, the mine hunting system performance is now driven by classification. The classification decision process, based on sonar images including shadows and echoes features, corresponds to the discrimination between MILCO (MIne Like Contact) and NON MILCO. This paper describes the operational incidence of a new theoretical approach used for shadow and image based classification performance evaluation. This approach is named DMC for Delta-Mask based Classification as it assumes the knowledge of specific objects images characteristics, represented with a specific statistical grid named the Delta-Mask. This theory leads to the computation of COC (Classification Operational Characteristics) curves, which give the probability of classification ( $P_c$ ) and the probability of false classification ( $P_{fc}$ ) as functions of sonar characteristics and operational conditions. These curves are computed for several types of sonar systems. Results based on real practical sonar images are shown and operational incidence is deduced.

## 1. INTRODUCTION

### 1.1 MINE HUNTING DECISION AND TERMINOLOGY

Classically, mine hunting is a three steps process: (1) detection, (2) classification and (3) identification (possibly followed by mine disposal).

Hence, the mine hunting operation can be described by the decision scheme on figure 1.

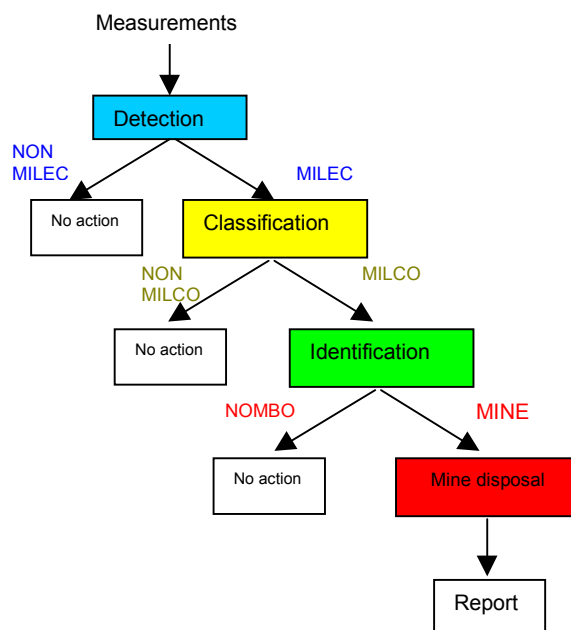


Figure 1 : Mine hunting decision scheme

The sonar measurements are filtered throughout a several stages decision process. The first stage is detection, which aims to decide whether there is a MILEC (Mine Like Echo) within the sonar field. This stage can be a one shot or a multi-ping detection process.

The second stage is the classification process. Measurements of each MILEC are analysed (complementary images or echoes can be obtained) to decide if the MILEC corresponds or not to a MILCO (Mine Like Contact).

The third decision stage is related to the identification of the MINE or the NOMBO (Non Mine Like Bottom Object). Identification aims to decide what sort of mine has been detected (MANTA, ROCKAN, MU80, ...) whereas classification aims only to decide if the detected echo is potentially a mine.

## **1.2 OPERATIONAL AND PRACTICAL CONTEXT OF CLASSIFICATION PERFORMANCE EVALUATION**

When mines still used to be high target strength objects, the number of non-mine objects passed on to the classification step was relatively small and, as a result, the overall mine hunting effort was mostly dimensioned by the detection process. This has rather drastically changed now that modern mines have become very stealthy ; Sonar systems, designed to detect them, will now also hand over to the classification process many more small non-mine bottom objects, with mine-like target strength. Hence, the classification process is now called upon much more often than it was in the past, hereby increasing its share in the overall mine hunting effort. Considering a number of several hundreds detected objects per square nautical mile it becomes necessary to classify the objects as rapidly and as securely as possible in order to limit the global time to fulfil the mine hunting mission.

To realise the classification step two solutions can be used. The first method is long range echo classification, which can be performed with a long range detection sonar by analysing the echo signal structure. The second method is image based classification, which uses a more detailed acoustic image of the object, including both echo structure and shadow shape, given by a classification sonar that has a better resolution. The second one is considered here.

The system performance at the output of the classification step can be evaluated by the residual risk (which is the probability that a mine within the field of operation had not been classified as MILCO, compared to an initial risk of mine presence) within a given operation time on a predefined operation theatre. The performance can be evaluated, dually, by the residual risk within an operation time, or by the operation time required to obtain a given residual risk.

Obviously, the overall performance of the mine hunting operation depends not only on the classification process performance but also on the overall optimisation and operational combination of the detection and classification sonar systems.

The performance of the detection process is defined by the probability of detection  $P_d$  of the sonar (parameter B of NATO standard) and the intercept of the sonar (parameter A of NATO standard) for a given probability of false alarm  $P_{fa}$ . The evaluation of  $P_d$  and  $P_{fa}$  is well known from the sonar community and is a classical standard of detection performance evaluation, for which, a detection index can be computed. This detection index is more or less a signal to noise ratio at the detection output. It facilitates immediate comparison of sonar systems in a given environment situation and a given mine threat.

Formerly, as classification was a rather episodic process of the mine hunting operation, it was not necessary to compute the efficiency of this step to determine the global performance of the mine hunting operation. However, as the classification process has become a more time consuming exercise and is today the most critical step of both detection and classification, the precise evaluation of its performance becomes mandatory.

## **1.3 OBJECT OF THE PAPER**

Despite some attempts to unify the standards of shadow classification performance evaluation (see Pinto [1] for example), the fact is that, practically, the usual requirements of classification sonar are summarised in a specified number of beams on the object (e.g. more than 3 or 4) and a given reverberation to shadow contrast (e.g. more than 5 dB).

In the following, a method is proposed, to evaluate the performance of the image based classification step, for a given sonar, in specific environmental conditions and a given mine threat. The method is described through its theoretical and practical aspects. The method infers the definition of a classification index that confirms the usual practical requirements for the sonar design. Examples of sonar performance are given and operational incidence is deduced.

## 2. PRINCIPLES OF SONAR IMAGE BASED CLASSIFICATION

### 2.1 DESCRIPTION OF THE CLASSIFICATION OPERATION

The classification process inputs are the measures associated to previous detected MILEC. A MILEC is the output of the detection phase. The MILEC corresponds to one of the following situation :

1. The MILEC is the echo of a mine
2. The MILEC is the echo of a non mine object (man made or natural)
3. The echo is a false alarm (noise or bottom scattering)

The classical theoretical false alarm situation of the detection operation is the third case. The two first cases correspond to correct detection cases. The classification phase aims to decide whether or not a mine is present, that is to discriminate mainly between case 1 and 2, knowing that case 3 (the detection false alarm situation) is a rather rare case due to common low false alarm detection threshold.

After detection, the classification process is based on a sonar image analysis that includes both echo and shadow contribution of the object.

The classification operation is described in figure 2 as a two hypothesis decision process. Considering this approach, the classification theory can be derived by today classical statistical mathematics for hypotheses testing (see Borovkov [2] or Kendhal & al [3] for instance). This is very similar to the two hypothesis decision process of the detection theory.

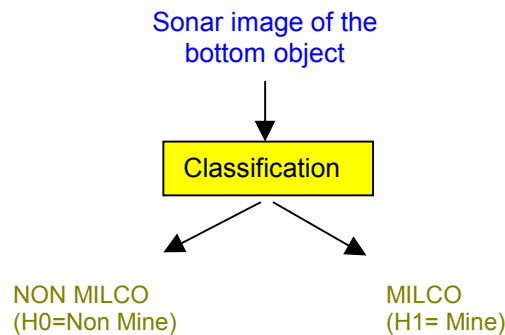


**Figure 2 : Classification decision process**

The difference with the detection stage lies in the input which is now a sonar image of the object and the two decisions which are MILCO ( $H_1 = \text{Mine}$ ) or NON MILCO ( $H_0 = \text{Non Mine}$ ).

### 2.2 DEFINITION OF THE COC CURVES

Assuming that parametric statistical models are defined to describe the measured image under the respective hypotheses  $H_0$  and  $H_1$ , the performance of the classification can be described by the COC curves (Classification Operational Characteristic curves) of the sonar. These curves draw the dependence between probability of classification ( $P_c$  is the probability to decide that the image corresponds to MILCO knowing that the object is a mine) and probability of false classification ( $P_{fc}$  is the probability to decide that the image corresponds to MILCO knowing that the detected object -in a wide sense that is including detection false alarms- is not a mine). COC curves are defined for a given sonar in well defined environmental conditions (grazing angle, range, reverberation level, shadowing, characteristics of NOMBO and false detection- see below) and for a specific mine. In fact, it is obvious that the probability of classification depends on the mine type as the probability of detection does too.

Evaluating  $P_c$  and  $P_{fc}$  requires the definition of not only the parameters of the sonar (wavelength, bandwidth, array size,...) but also of the implemented classification algorithm. This algorithm is not easily accessible, not only because sonar designers keep it secret, but also because its statistical model is not easily analytically derived ; The algorithm performance depends on the mine and non mine on board data base knowledge, and on the operator ability, knowing that, classification is most often an "operator in the loop" process. So, only the case where the classification algorithm is a near-optimal test derived from the Neyman-Pearson optimal decision test is considered. In that case, considering the sonar ability to classify mines, sonar design parameters can be compared in an unbiased perspective, assuming that the decision algorithms and software are designed for reaching more or less a kind of optimal strategy, based on a referenced data base.

The evaluation of the classification process requires the possession of a model and a data base of measurements from mine and non mine objects. These model and data base shall be use to define and test the decision process in a statistical sense.

The model includes both the pure acoustic behaviour of the object in its environment and the transfer function of the measurement sonar equipment. The evaluation of the probability of classification and of the probability of false classification in a given situation is performed using model and data base.

### 3. STATISTICAL DECISION MODEL

#### 3.1 SONAR IMAGE AND MASK MODEL

The principle of sonar imaging is the contribution of bottom reverberation and the appearance of acoustic shadows behind the object.

A sonar image contains namely three kinds of pixels : reverberation, echoes, shadow (see figure 3).

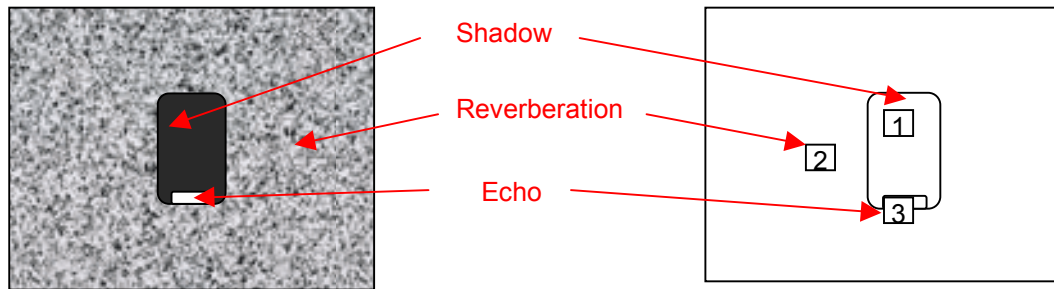


**Figure 3 : Pixels categories of a sonar image**

Each pixel category can be given a statistical distribution function or equivalently a probability density function. This function describes the statistical behaviour of the pixel, that is, roughly, the probability that the pixel takes its numerical values within a given interval.

It is assumed that the distribution functions of the pixels are chi-squared distributions, also known as the generalised Rayleigh, Rayleigh-Rice or Rice distributions. This hypothesis is usual for sonar imaging and can be deduced from some classical gaussian hypotheses about echoes, noise and reverberation signals.

Considering that the beams and range gates of the sonar image are sampled with the sonar resolution in both range ( $C/2B$ ,  $C$  = sound speed ;  $B$  = Sonar Bandwidth) and bearing ( $\lambda/L$  ;  $\lambda$  = wavelength,  $L$  = array length), it can be assumed that the pixel statistics are independent. This is of high importance for the following. Increasing the number of pixels by over sampling the range or beam dimensions does not increase the statistical information contained in the image. This usual over sampling process is mainly required for "operator comfort" or for finer estimation of shadow borders or echoes positions. The over sampled image can be reconstructed using the "raw pixels", which are the pixels sampled with the sonar resolution. So, in the following, it is considered that the image is a "raw image", that is an image sampled with a rate corresponding to sonar resolution in range and bearing (independent range gates and independent bearings).

Assuming that one knows the object and sonar characteristics, the associated theoretical statistics of the pixels can be determined. Each pixel can belong to one of the following statistical law :

- Bottom reverberation  $p_1(x)$
- Shadow  $p_2(x)$
- Echo  $p_3(x)$
- Undetermined  $p_{-}(x)$

The statistical behaviour of an image can be represented with a 2D mask (or grid). Each square of the grid corresponds to a pixel of the image and includes the index number of the statistical law associated to this pixel (see figures 3 and 4).

2	2	2	2	2	2	2	2	2	2	2
2	2	2	2	2	2	2	2	2	2	2
2	2	2	2	1	1	1	2	2	2	2
2	2	2	2	1	1	1	2	2	2	2
2	2	2	2	1	1	1	2	2	2	2
2	2	2	2	1	1	1	2	2	2	2
2	2	2	2	3	3	3	2	2	2	2
2	2	2	2	2	2	2	2	2	2	2
2	2	2	2	2	2	2	2	2	2	2

**Figure 4 :**

**2D mask symbolising the image of figure 3**

### 3.2 STATISTICAL DECISION TEST AND DELTA-MASK

Using the theoretical mask of a known object in hypothesis H1 (if the object is the mine) or H0 (if it corresponds to a NOMBO or a detection false alarm) and assuming that the pixels are independent, the probability density function of the image can be written as the product of the probability density functions of its pixels. So the Neyman-Pearson hypothesis test comes down to :

$$\prod_{i,j} \frac{p(x_{ij} / H_1)}{p(x_{ij} / H_0)} \underset{o}{\overset{1}{\geq}} \underset{o}{\overset{1}{<}} Threshold \quad (1)$$

where  $x_{ij}$  is the pixel value of row  $i$  and column  $j$ .

Due to the pixels statistical independence hypothesis this test has the interesting property that the product can be limited to the set of pixels  $(i, j)$  corresponding to different statistical behaviours for H0 and H1. Hence, when the statistical density of a given pixel is the same under the hypothesis H1 and under the hypothesis H0, the contribution of this pixel to the product in equation (1) is a factor equal to 1 (that is, there is no information coming from this pixel for testing).

So, the previous test can be limited to what can be named the delta-mask, that is the mask of pixels corresponding to different statistical laws under H1 and H0. As an example, the delta mask of the two "symbolic" shadows ring and square, as described in Pinto [1], is given on figure 5.

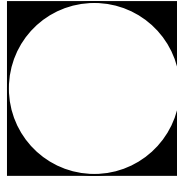


**Figure 5 : Example of a delta mask between a square and a ring**

The delta-mask determination sets the problem of centring the shadows under H0 and H1, for determining the correct delta-mask. Centring is in fact a common operation in sonar image classification which is implicitly or explicitly realised (See for examples Quidu and al [4] or Fawcett [5]). In fact, a lot of technical processes exist to centre shadows of objects (including or not echoes contributions). For instance, the centre of a mask could be referred to the centroid (or centre of mass), the density weighted centroid or the geometric centre as described in Costa and Cesar [6] or Russ [7]. For the determination of the delta-mask, it is preferred here to centre the two masks by choosing the delta-mask which minimises the number of its pixels (more refined techniques could be searched amongst likelihood maximisation approach or mini-max criteria as we know the likelihood function, but it would lead probably to somehow similar results).

So the effective optimal test for a given delta-mask  $\Delta$  is expressed by the following equation (2).

$$\prod_{i,j \in \Delta} \frac{p(x_{ij} / H_1)}{p(x_{ij} / H_0)} \underset{o}{\overset{1}{\geq}} \underset{o}{\overset{1}{<}} Threshold \quad (2)$$

A given delta mask  $\Delta$  is divided in six sub-masks  $\Delta^{12}, \Delta^{13}, \Delta^{21}, \Delta^{23}, \Delta^{31}, \Delta^{32}$ . For a sub-delta mask  $\Delta^{kl}$ ,  $k$  and  $l$  represent the statistical category of the pixel for the NOMBO and for the MINE respectively. This category can be 1=shadow, 2=reverberation, 3=echo. The sub-masks  $\Delta^{11}, \Delta^{22}, \Delta^{33}$  and the undetermined pixels are of no interest, because they don't contribute to the statistical decision.

For example, the masks of a NOMBO (rock), a MANTA MINE, and the corresponding sub-masks  $\Delta^{21}$  and  $\Delta^{12}$  are given on figure 6a to 6d. The echo effects are not taken into account in this example ; focus is made here on pure shadow classification.

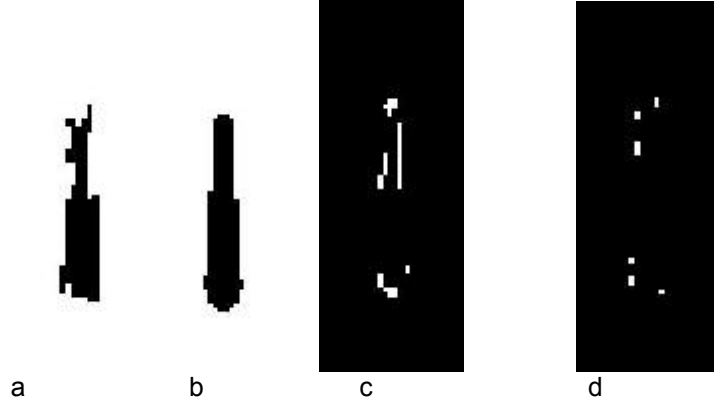


Figure 6 : Examples of NOMBO (a), MINE (b),  $\Delta_{21}$  (c) and  $\Delta_{12}$  (d) masks

Assuming that the basic pixels statistical distributions are chi-squared distributions, it can be shown that equation (2) is equivalent to the following test :

$$\sum_{\substack{k,l \\ k \neq l}}^{3,3} (\alpha_h^{kl} \cdot \chi_{2N^{kl}}) \begin{matrix} \geq \\ < \\ 0 \end{matrix} \begin{matrix} 1 \\ \\ \end{matrix} Threshold_{bis} \quad (3)$$

where  $N^{kl}$  is the number of pixels of the sub-mask  $\Delta^{kl}$ ,  $\chi_{2N^{kl}}$  is a chi-square variable with a  $2N^{kl}$  degrees of freedom, and  $\alpha_h^{kl}$  is a set of real coefficients depending on the measured mean powers of noise (shadow), reverberation and echoes. The index  $h$  is the index of the basis hypothesis H0 or H1, that is  $\alpha_h^{kl}$  varies as a function of hypothesis H0 or H1. In fact,  $\alpha_h^{kl}$  is defined by :

$$\alpha_0^{kl} = \left( \frac{\gamma^l - \gamma^k}{\gamma^l} \right) \quad (4)$$

$$\alpha_1^{kl} = \left( \frac{\gamma^l - \gamma^k}{\gamma^k} \right) \quad (5)$$

where  $\gamma^k$  is the received signal power associated to one pixel ( $E(x_{ij})$ , when  $x_{ij}$  is the sum of two square of normal variables, as being the output of a quadratic detector) for shadow ( $k=1$ ), reverberation ( $k=2$ ) or echo ( $k=3$ ).

A shadowing effect, as produced by sand ridges, can be taken into account by suppressing some pixels of the delta-mask in equation (3).

### 3.3 COC CURVES COMPUTING

Using common statistical inferences on chi-square variables the COC-curves corresponding to equations (3), (4) and (5) can be easily computed, either with Monte-Carlo techniques or with numerical derivation of analytical equations. For example it can be shown that the distribution function of the statistical variable of equation (3) can be computed as linear combination of a set of chi-square distributions :

$$Pr ob \left\{ \sum_n \alpha_n \chi_{2N_n}^2 < x \right\} = \sum_n \sum_{s=1}^{N_n} \beta_{ns} Pr ob \left\{ \chi_{2s}^2 < \frac{x}{\alpha_n} \right\} \quad (6)$$

where the coefficients  $\alpha_n$  and  $\beta_{ns}$  can be computed.

For the example of masks given on figures 6, the COC curve can be easily computed, for a given reverberation to shadow contrast,  $10 \log \left( \frac{\gamma^1 - \gamma^0}{\gamma^0} \right)$ , equal to 5 dB. The curves refers to sonar A, B and C (see paragraph 4 below) and are given on figure 7.

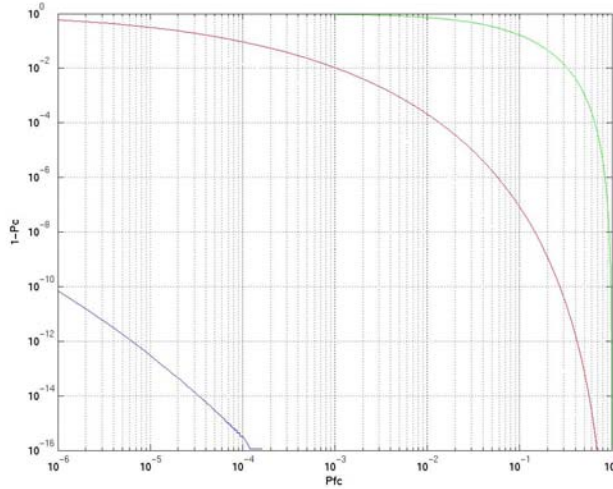


**Figure 7 : COC curves for sonars A (green), B (red), C (blue), 5dB reverberation to shadow contrast and the delta-mask of figure 6.**

So, it is obvious, that, for given SONAR characteristics (range and beam resolutions, grazing angle, noise, reverberation, and echoes measured powers), a given MINE and a given NOMBO, the related COC curve can be computed, which gives the maximal performance of the classification capability of the sonar.

### 3.4 CLASSIFICATION INDEX

Using a similar approach to that adopted in detection theory, by making a gaussian approximation, it can be shown that a specific index characterises the COC curves. The general expression of this index is given in equation (7).

$$I_c = \frac{\sum_{k,l} N^{kl} (\alpha_1^{kl} - \alpha_0^{kl})}{\sqrt{\sum_{k,l} N^{kl} \alpha_0^{kl} \alpha_0^{kl}}} \quad (7)$$

Assuming that the general performance of the sonar can be deduced from the discrimination problem between a ring and a square, as Pinto [1] assumed, and as illustrated on figure 5, the following expression of the classification index of a sonar can be given in equation (8).

$$I_{C (dB)} = C_{R/S (dB)} + 5 \cdot \text{Log}_{10} \left( \frac{s}{\delta \frac{c}{2B}} \right) + 10 \cdot \text{Log}_{10} \left( \frac{\cos \phi}{\sqrt{\sin \phi}} \right) - 3.4 \text{dB} \quad (8)$$

where  $c$  is the sound velocity in water (m/s),  $B$  is the sonar bandwidth (Hz),  $\delta$  is the sonar beam-width resolution on the object in metres,  $s$  is the object cross section in square-metres,  $\phi$  is the grazing angle,  $C_{R/S}$  is the reverberation to shadow contrast.

## 4. PRACTICAL APPLICATION

### 4.1 VARIABILITY OF MASKS AND SITUATION

During a mine hunting operation the sonar can face a wide variety of situations including various MINE masks and NOMBO masks.



Even for a single mine, the variations of the position of the mine on the sea bed, and so the variations of relative positions to the sonar and the bottom, lead to variations of the mine masks for a same operational hypothesis. For instance, a ROCKAN mine induces a wide variety of masks, due to the wide variety of projected shapes, induced by a simple rotation of the mine around its vertical axis. Variations of ROCKAN masks are illustrated on figure 8a, 8b, 8c.



**Figure 8 : (a) (b) (c) various shadow masks of a ROCKAN mine simulated at a grazing angle of 13 degrees**

Considering the natural variability of natural or man made bottom objects, the same sonar can meet a large number of NOMBO types of various size, shapes and asymmetric forms, that induces a large number of NOMBO hypothesis. In fact, for our performance evaluation, the natural principle of diversity leads to a large number of NOMBO possible masks. The bottom can be associated to a set of possible NOMBO masks. For convenience, the masks can be normalised to a reference grazing angle.

#### 4.2 STATISTICAL MIXTURES OF MASKS AND TEST EVALUATION

For given sonar characteristics (range and beam resolutions, grazing angle, noise, reverberation, and echoes measured powers), the statistical variable representing the mine image and the statistical variable representing the NOMBO image are to be considered as statistical mixtures (for more information on statistical mixtures in the gaussian case see for instance Plataniotis & Hatzinakos [8]). Equation (4) shall be adapted to take into account this mixture situation.

The mixture can be represented by a set of delta-masks. Each delta-mask of the set corresponds to the association of a particular MINE mask with a particular NOMBO mask. Each delta-mask is given a mixing coefficient (weight  $q_n$ ). This coefficient  $q_n$  represents a kind of probability of occurrence of the decision to be concerned by the situation of this MINE mask against that NOMBO mask. The adaptation of equation (4) to the mixing problem gives the following equation (9), where  $n$  is the index over the delta-mask set.

$$\sum_{\substack{k,l \\ k \neq l}}^3 \left( \alpha_h^{k \ln} \cdot \chi_{2N^{k \ln}} \right) \begin{matrix} \geq \\ < \\ 0 \end{matrix} \begin{matrix} 1 \\ \\ \end{matrix} \text{Threshold}_n \text{ with probability } q_n \quad (9)$$

It is also assumed that, in this decision process, all the thresholds are determined in order to let the probability of false classification  $Pfc_n$  being the same for all the tests of the set. In that case, the global probability of classification  $Pc$  is the weighted mean of the probabilities of classification  $Pc_n$  of the individual decision tests of the set.  $Pfc$  and  $Pc$  are determined by the following equations (10) and (11) :

$$Pfc = Pfc_n \quad (10)$$

$$Pc = \sum_n q_n \cdot Pc_n \quad (11)$$

Hence, the global COC curve of the classification test is the weighted mean of the COC curves associated to the different delta-masks of the set.

#### 4.3 EXEMPLE OF OPERATIONAL EVALUATION OF CLASSIFICATION

In order to illustrate the application of the previous theory, an example of evaluation of the classification performances of different sonar systems is studied for a given operational bottom theatre. To do so, a set of NOMBO masks has to be first determined, that represents the possible operational situation. The determination of the NOMBO masks is made by the use of the side scan sonar image given in figure 9. This image has been recorded by the GESMA with a DUBM41 side scan sonar. It shows a bottom situation with a lot of bottom objects.

The objects of the image, are detected and the associated masks are computed and normalised for a reference grazing angle. Too small objects have been eliminated and masks include only shadow contributions. In this example, no echo contribution is taken into account. Afterwards, a clustering algorithm is used to elaborate different classes of masks over the set of the detected objects. Each class is parameterised with a specific class centroid and complementary synthetic masks are generated using the class centroid models in order to add masks to the data base.

Figure 10 gives a 2D representation of the data base. Each object is represented by a marker on a 2D grid. The x-axis represents the shadow width and the y-axis represents the shadow length. The units are the numbers of pixels of the original image at the reference grazing angle (mean grazing angle). Each marker can represent several objects. In fact, the data base contains a total of 289 NOMBO shadow masks. The masks are assumed to be equi-probable (that is to have the same likelihood of occurrence).



**Figure 9 : Original side scan sonar image**

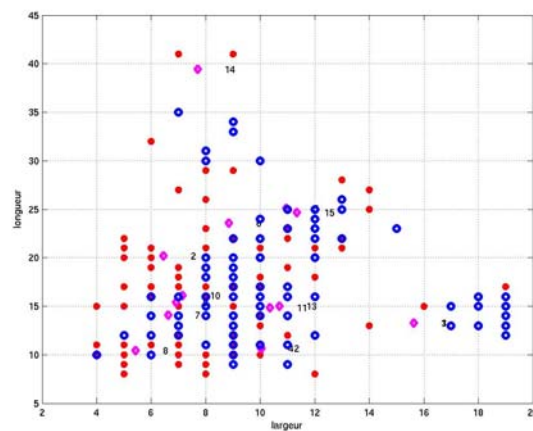


**Figure 10 - 2D representation of the NOMBO data base (original data = red, class centroids =pink, synthetic data = blue)**

Using the previous data base and equations (7) and (8), the COC curve is computed for a MANTA mine and for three different sonar systems. The three systems are assumed to have the same range resolution. They only differ in their beam width. Sonar A (in green) has a resolution of 2.2 beams on the mine, Sonar B (in red) has 3.3 beams and Sonar C (in blue) has 6.6 beams. The COC curves are computed for two levels of reverberation to shadow contrast, 5dB and 2 dB, and drawn on figures 11 and 12 respectively.

These curves can be interpreted in an operational way. The x-axis corresponding to Pfc is a direct evaluation of the operational efficiency of the classification. Pfc represents the proportion of NOMBO objects that will be classified as MINE. Each such false classification will lead to a starting of an identification operation. This identification will slow down the global mine hunting operation. In fact Pfc has to be chosen in relation with the MILEC density (i.e. number of detected NOMBO per square mile) and with the global time period allocated to the mine hunting operation. The y-axis corresponding to 1-Pc is a direct evaluation of the operational risk of the classification. 1-Pc represents the proportion of MINES that will be classified as NOMBO. This risk is of course critical as it represents the number of missed mines.

In the given example, if it is assumed that the residual risk must be less than 1‰, the curves show that sonar A and sonar B cannot be used with a sufficient efficiency. If a residual risk of 1‰ is accepted, sonar B can be used with a 3% efficiency. So, using this sonar, requires to identify three percent of the detected NOMBOs. While using sonar C, even with a bad contrast of 2dB, a residual risk of less than 0.1‰ can be obtained with 3% efficiency.

## 5. ACKNOWLEDGEMENT

The work presented here was realised under the French Government DGA (Délégation Générale pour l'Armement) A 99 77 120 contract number. The authors thanks very much DGA/SPN (Service des Programmes Naval) that supported the study and DGA/GESMA (Groupe d'Etudes Sous-Marines de l'Atlantique) that provided the sonar image in order to elaborate the NOMBO data base.

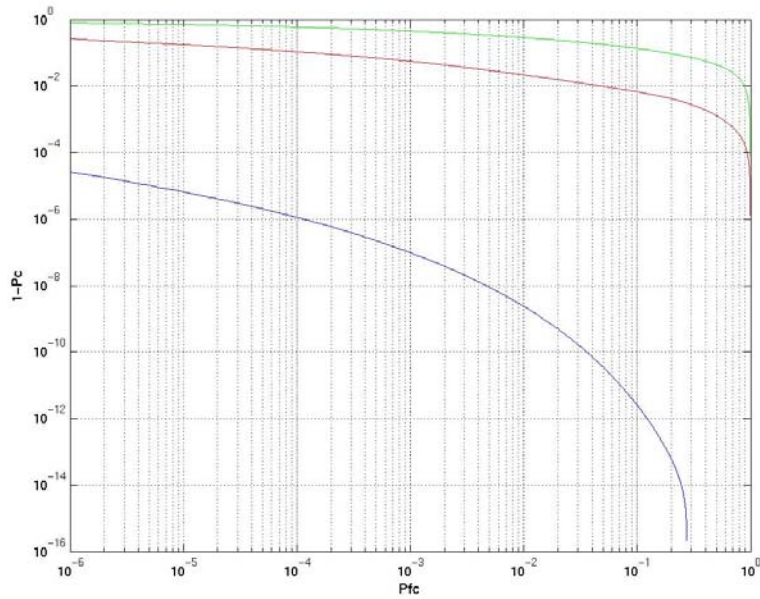


Figure 11 : COC curves - CR/S=5dB

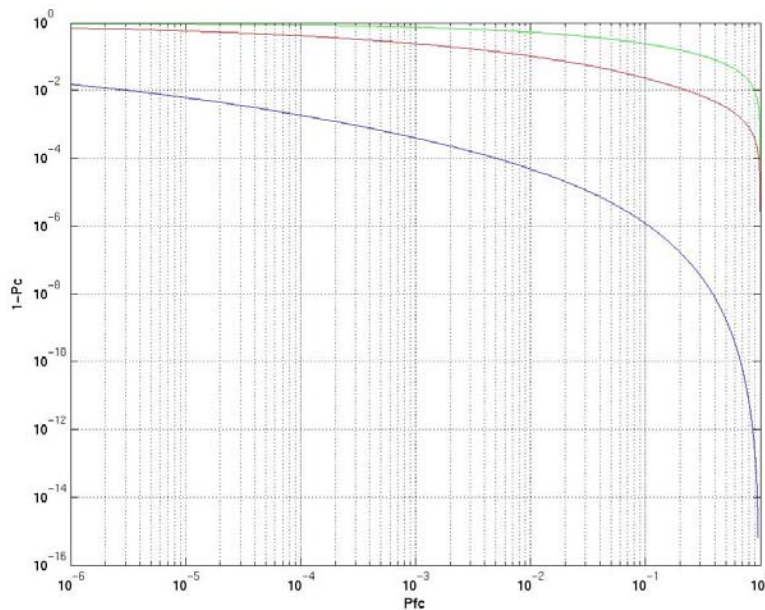


Figure 12 : COC curves - CR/S = 2 dB

## 6. CONCLUSION

A method to evaluate the performance of classification sonar systems has been introduced. This DMC (Delta-Masks Classification) method uses all the available knowledge concerning the mines and the non mine bottom objects (NOMBOs) in the environment. It can be adapted to any bottom type, provided that, a NOMBO data base has been created for the bottom type. Such a data base can be made from the analysis of data extracted from a high resolution sonar image of the zone.

The DMC method can be adapted to take into account the presence of shadowing effects as created by sand ridges. As this method is elaborated with optimal decision tests (Neyman-Pearson criteria), it allows to really compare the classification capability associated to sonar design, with no operator influence. A classification Index has been determined, that summarises the classification capability of the sonar. This index depends on the reverberation to shadow contrast, the 2D sonar resolution compared to the object cross section, and the grazing angle. An example of COC curves computation has been given. The method has now to be tested out in various bottom conditions and for different sonar systems and different mine threats.

## 7. REFERENCES

- [1] M. A. Pinto, Performance index for shadow classification in minehunting sonar, 24-26 June 1997, Proceedings UDT 97, Hambourg Congress Centre, Germany, pp. 159-163,
- [2] A. Borovkov, Statistique Mathématique, Ed. MIR, TR, Moscow, 1987,
- [3] Sir M. Kendhal, A. Stuart, and J. K. Ord, The advanced theory of statistics, Volume 3, Design and analysis, and time-series, Fourth Edition, Charles Griffin & Company limited, London & High Wycombe, 1983.
- [4] I. Quidu, J. Ph. Malkasse, G. Burel, and P. Vilbé, "Mine Classification based on raw sonar data: an approach combining Fourier descriptors, statistical models, end genetic algorithms", Providence, Proceedings of Oceans 2000.
- [5] J. A. Fawcett, Image-based classification of sidescan sonar detections, Proceedings of CAD/CAC 2001, Halifax, Nov. 12-14, 2001.
- [6] L. da Fountura Costa, R. Marcondes Cesar Jr., Shape Analysis and Classification, Theory and Practice, CRC Press, 2001, p. 425.
- [7] J. C. Russ, The image Processing Handbook, Fourth Edition, CRC Press, 2002, pp. 481 -484.
- [8] K. N. Plataniotis, D. Hatzinakos, in Advanced signal processing handbook; CRC Press, S. Stergiopoulos Ed., 2001, pp.3.1-3.35